Cambridge Prisms: Extinction

www.cambridge.org/ext

Demographic synchrony increases volatility and extinction risk in human populations

Marcus John Hamilton[1,2,3] and Robert Walker[4,5]

[1]Anthropology, The University of Texas at San Antonio, USA; [2]Santa Fe Institute, USA; [3]Center for Data Science, University of Texas at San Antonio, San Antonio, USA; [4]Anthropology, University of Missouri, USA and [5]Center for Applied Statistics and Data Analysis, University of Missouri, Columbia, USA

Research Article

Cite this article: Hamilton MJ and Walker R (2026). Demographic synchrony increases volatility and extinction risk in human populations. *Cambridge Prisms: Extinction*, **4**, e8, 1–10
https://doi.org/10.1017/ext.2026.10013

Received: 08 October 2025 UTC
Revised: 10 March 2026 UTC
Accepted: 12 April 2026 UTC

Keywords:
vulnerability; stability and collapse; prehistoric; population size; demographic stochasticity

Corresponding author:
Marcus John Hamilton;
Email: marcus.hamilton@utsa.edu

Abstract

Cooperation is widely viewed as a stabilizing force because it pools risk and buffers against environmental uncertainty. Demographic theory predicts that volatility in per-capita population growth declines rapidly with population size, implying that larger populations should be more stable. Yet human societies of all sizes eventually collapse. Here, we propose a general mechanism that helps explain this pattern. We show that cooperation generates demographic synchrony—correlated survival and reproductive outcomes among individuals—which inflates aggregate volatility. Using more than 200 longitudinal population records from indigenous societies in the Brazilian Amazon, we find that volatility declines with population size substantially slower than predicted under demographic independence. This pattern implies pervasive within-population correlation, such that census populations behave demographically as if composed of far fewer independent modules. We formalize this process with a synchrony-extended stochastic model in which shared environmental exposure, social coupling, and spatial overlap generate demographic correlations that erode the stabilizing effects of scale. We term this dynamic the *cooperation–synchrony paradox*: the same institutions that reduce risk for individuals can increase vulnerability to population-wide shocks. Further, we propose this is likely a general mechanism across species, where cooperation stabilizes locally but generates systemic fragility by reducing effective demographic dimensionality.

Impact statement

Cooperation is one of the most powerful strategies in the evolution of life. By sharing resources, coordinating behavior and pooling risk, cooperative organisms, from social insects to human societies, reduce individual vulnerability to environmental uncertainty. Classical demographic theory, therefore, predicts that larger populations should become increasingly stable because random fluctuations in births and deaths average out as populations grow. Yet the historical and ecological record repeatedly contradicts this expectation. Large populations sometimes experience dramatic demographic collapses despite appearing robust. This study addresses that paradox. Drawing on more than 200 time series of indigenous populations in the Brazilian Amazon, we show that population volatility declines with size far more slowly than predicted by classical demographic models. This deviation indicates that individuals within populations are not demographically independent. Shared ecological conditions, cooperative institutions, social networks and spatial overlap synchronize survival and reproduction across individuals, producing correlated modular demographic outcomes within populations. We refer to this dynamic as the cooperation–synchrony paradox. Cooperation stabilizes individuals by reducing idiosyncratic risks, but it simultaneously couples demographic outcomes across group members. As these correlations increase, the effective number of independent demographic units in a population declines. Populations, therefore, fluctuate with fewer degrees of freedom, weakening the stabilizing effects of scale and increasing vulnerability to large shocks. These results have implications well beyond Amazonian populations. By linking human demography with ecological synchrony theory, the study reveals a general constraint on the resilience of cooperative systems. Population size alone does not guarantee stability when demographic fates are shared. Understanding how cooperation reshapes demographic dynamics is therefore essential for explaining the persistence, fragility and collapse of complex social systems across the tree of life.

Introduction

Cooperation is one of the most powerful evolutionary strategies in the history of life (Nowak, 2006). Across taxa, cooperative organisms, from eusocial insects to cooperative breeding birds and mammals – including human societies – achieve ecological success through collective action

© The Author(s), 2026. Published by Cambridge University Press. This is an Open Access article, distributed under the terms of the Creative Commons Attribution licence (http://creativecommons.org/licenses/by/4.0), which permits unrestricted re-use, distribution and reproduction, provided the original article is properly cited.

Downloaded from https://www.cambridge.org/core. UNIVERSIDAD AUTONOMA METROPOLITANA, on 18 Nov 2026 at 04:05:37, subject to the Cambridge Core terms of use, available at https://www.cambridge.org/core/terms. https://doi.org/10.1017/ext.2026.10013

(Krause and Ruxton, 2002; Rubenstein and Lovette, 2007; Schindler et al., 2010; Bowles and Gintis, 2011; Rubenstein, 2011; Clutton-Brock, 2016). By pooling resources, sharing risk and coordinating behavior, cooperation reduces individual variance in survival and reproduction and enables populations to persist in complex stochastic environments. Yet cooperative systems are also prone to sudden collapse: colonies fail, packs disappear and societies crash despite appearing demographically robust (Lande, 1993; Tainter, 1988; Morris and Doak, 2002; Diamond, 2011; Turchin, 2018). This raises a fundamental question that spans ecology, evolution and anthropology: how can cooperation both stabilize and destabilize populations?

The human past provides a dramatic illustration of this tension, where societies repeatedly grow in scale only to undergo demographic collapse from some combination of internal and external processes (Tainter, 1988; Currie et al., 2010; Diamond, 2011; Walker and Hamilton, 2011; Butzer, 2012; Hamilton et al., 2014; Walker and Hamilton, 2014; Hamilton and Walker, 2018). Indeed, societal collapse is a recurrent process in cultural evolution and plays a major role in human demographic history (Cumming and Peterson, 2017; Hamilton and Walker, 2018; Gurven and Davison, 2019). While collapse is often framed in political or institutional terms, its ultimate manifestation is a demographic sudden reduction in population viability. In this article, we use the term "collapse" strictly in this demographic sense to refer to situations where fluctuations in births, deaths or migration push populations below some critical threshold from which recovery is unlikely (Shaffer, 1981; Lande, 1993; Morris and Doak, 2002; Lande et al., 2003).

Classical demographic theory predicts that larger populations should be increasingly stable. If births, deaths and migrations are independent stochastic events, volatility in per-capita growth rates declines as $\sigma(r) \propto N^{-1/2}$ (Shaffer, 1981; Lande et al., 2003; Keyfitz and Caswell, 2005). Thus, under this assumption, the law of large numbers guarantees that scale generates stability by rapidly averaging out stochasticity, and so volatility declines with scale. Yet these population dynamics seem to be constantly violated as large populations collapse while small populations sometimes persist.

Ecologists have long recognized that spatial synchrony undermines stability (Lande et al., 1999). When populations fluctuate together due to the shared environmental forcing of the Moran effect, dispersal coupling, trophic interactions or shared pathogens (Koenig, 2002; Liebhold et al., 2004; Moran, 1953; Bjørnstad et al., 1999), regional extinction risk increases because rescue effects weaken (Brown and Kodric-Brown, 1977; Earn et al., 1998; Hanski, 1999). However, synchrony is typically studied among subpopulations within metapopulations, and far less attention has been given to synchrony *within* populations, particularly in cooperative organisms.

In cooperative systems, individuals do not experience demographic events independently. Individuals share resources, exposure to pathogens, reproductive opportunities and social networks. Cooperative breeding, shared childcare, collective foraging and coordinated mobility couple individual fates. These forms of social integration introduce correlations in survival and reproduction, increasing covariance among demographic outcomes. As covariance rises, populations no longer behave demographically as collections of independent individuals. Instead, populations fluctuate with fewer degrees of freedom.

We term this demographic tension the *cooperation–synchrony paradox*. Cooperation evolves to buffer individuals against risk, reducing idiosyncratic variance in fitness-related outcomes. Yet the mathematical consequence of pooling risk is the creation of shared exposures and shared outcomes, which build demographic synchrony. Synchrony inflates group-level volatility by reducing the effective demographic degrees of freedom in a population. In a synchrony-extended model, populations behave not as N independent individuals but as $K(N)$ effective demographic "clusters," where K grows more slowly than N. As synchrony increases, the law of large numbers weakens, and volatility declines more slowly with scale than classical theory predicts. Cooperation stabilizes individuals while potentially increasing vulnerability at the population level by increasing modularity.

We investigate this paradox using a unique dataset of more than 200 time series of indigenous Amazonian populations compiled from Brazilian government censuses and historical records (see §3 for details). These small-scale societies represent modular, kin-structured and spatially bounded cooperative systems. Across 1,579 census observations and 1,353 growth intervals, we are able to measure volatility in per-capita growth rates and examine how stability scales with population size. These data provide a rare–perhaps anthropologically unique–opportunity to quantify demographic synchrony in small-scale human societies and to test whether the stabilizing effect of scale operates as classical models predict.

By bridging human demography with ecological theory, we argue that demographic synchrony represents a general constraint on the resilience of cooperative organisms. Just as synchrony among subpopulations elevates regional extinction risk in metapopulations, demographic synchrony among individuals elevates risk within single populations by inflating volatility. The Amazonian case serves not merely as a historical example of vulnerability, but as a tractable empirical system for understanding how cooperation reshapes the statistical structure of demographic processes.

First, we develop the mathematical framework for demographic synchrony. We then describe the data and estimation procedures and go on to present empirical estimates of volatility scaling and synchrony parameters and discuss data limitations. Finally, we explore the implications for cooperative organisms more broadly, arguing that demographic synchrony may represent an underappreciated source of fragility in social systems across the tree of life, and summarize these findings.

The model

Definitions and setup

We begin by defining variables where i indexes an individual population (or human society) and t indexes time steps (e.g., years). Let $N_{i,t}$ be a census size of the ith population at the time t. $A_{i,t}$ is the total geographic area associated with that population. It follows then that the population density of the ith population at the time t is $D_{i,t} \equiv N_{i,t}/A_{i,t}$. The instantaneous growth rate of the ith population at the time t is then $r_{i,t} \equiv \ln(N_{i,t+1}/N_{i,t})$.

Baseline demographic stochasticity

Under the demographic-noise baseline, individuals are assumed to act independently, and the annual probability of an individual reproducing is statistically independent. As such, net demographic increments are approximately Poisson with variance proportional to N (Shaffer, 1981). Let $\Delta N_{i,t}$ denote the net increment with variance $\mathrm{Var}(\Delta N_{i,t}) = v N_{i,t}$. Since $r_{i,t} \approx \Delta N_{i,t}/N_{i,t}$ for small increments, we obtain the well-known scale-dependent relationship

Downloaded from https://www.cambridge.org/core. UNIVERSIDAD AUTONOMA METROPOLITANA, on 18 Nov 2026 at 04:05:37, subject to the Cambridge Core terms of use, available at https://www.cambridge.org/core/terms. https://doi.org/10.1017/ext.2026.10013

$$\mathrm{Var}(r|N) \approx \frac{v}{N} \propto N^{-1}, \Rightarrow \sigma(r|N) \approx \sqrt{\frac{v}{N}} \propto N^{-1/2}. \quad (1)$$

Equation 1 is the demographic baseline expectation, where demographic volatility decays as $N^{-1/2}$ under demographic independence.

A synchrony-extended model

The observed per-capita growth rate of a population is the average of many individual contributions. Let $y_{ij,t}$ denote the demographic contribution of the individual j in population i at time t to the change in population size between t and $t+1$. Each $y_{ij,t}$ is a random variable representing the stochastic outcome of demographic processes such as survival, birth, death or migration. For instance, survival without associated change contributes $y_{ij,t} \approx 0$, death or out-migration contributes $y_{ij,t} < 0$ and birth or in-migration associated with the individual j contributes $y_{ij,t} > 0$.

Formally, we assume

$$\mathbb{E}\left[y_{ij,t}\right] = \mu_i, \quad \mathrm{Var}\left(y_{ij,t}\right) = s^2,$$

We introduce pairwise correlation $\rho_{i,t}$ across individuals within the same population:

$$\mathrm{Corr}\left(y_{j,t}, y_{k,t}\right) = \rho \quad \text{for} \quad j \neq k.$$

The per-capita growth rate is then the average of the individual demographic contributions across the population

$$r_{i,t} = \frac{1}{N_{i,t}} \sum_{j=1}^{N_{i,t}} y_{ij,t}. \quad (2)$$

and the conditional variance of the per-capita growth rate in this synchrony-extended model is then

$$\mathrm{Var}(r|N) = \frac{1}{N_{i,t}^2} \mathrm{Var}\left(\sum_{j=1}^{N_{i,t}} y_{ij,t}\right) = \frac{s^2}{N_{i,t}} \left[1 + (N_{i,t} - 1)\rho_{i,t}\right]. \quad (3)$$

If $\rho_{i,t} = 0$, we recover the demographic baseline $\sigma(r) \sim N^{-1/2}$, whereas if $\rho_{i,t} > 0$, volatility falls more slowly with N.

Statistical estimation of scaling parameters

We then wish to use data to estimate the parameters of the volatility scaling law we just derived:

$$\sigma(r|N) = cN^{-\alpha}. \quad (4)$$

We proceed as follows. First, population sizes are grouped into exponentially increasing bins along the N-axis, with bin sizes $N_{\mathrm{bin}} = 1,2,4,8,16,32,\ldots$. Estimating the scaling relation given by equation 4 requires systematically measuring the change in standard deviation of the growth rate as the population increases in scale. Exponential binning of N ensures that each scale of population size is equally represented in the analysis. Because the distribution of N is typically right-skewed, with many small populations and relatively few large ones, equal-width bins would overweight small populations and underweight large ones. Exponential bins balance the representation of different scales, stabilize variance estimates within bins and ensure that the regression on $\ln N$ is not dominated by the smallest populations. This procedure is standard in scaling analyses of fluctuations (Stanley et al., 1996).

For each bin, we collect all observed growth rates $r_{i,t}$ from populations whose size $N_{i,t}$ falls within that bin, and compute the empirical standard deviation

$$\widehat{\sigma}(r|N_{\mathrm{bin}}) = \sqrt{\mathrm{Var}\{r_{i,t} : N_{i,t} \in N_{\mathrm{bin}}\}}.$$

This yields a binned set of estimates across the population-size distribution. We then fit the log-linearized scaling relation

$$\ln \widehat{\sigma}(r|N) = \ln c - \alpha \ln N_{\mathrm{bin}} + \varepsilon, \quad (5)$$

where $\ln c$ is the intercept, α is the slope and ε is an error term. Ordinary least squares regression of $\ln \widehat{\sigma}(r|N)$ on $\ln N$ provides point estimates of c and α, while the dispersion of residuals provides confidence intervals. In this framework, c represents the baseline volatility at $N = 1$, and α quantifies the rate at which volatility decays with population size.

Materials and methods

Demographic data collection

We compiled our dataset from the (Instituto Socioambiental, 2025), including sources (Ricardo and Ricardo, 1986, 1991, 1996, 2000, 2006, 2011, 2016, 2023). These are population census estimates of recently contacted indigenous populations throughout Brazil collected over many generations. These sources provided 1,580 individual census estimates for 227 populations, with the earliest estimate from 1749 and the most recent from 2023. Population sizes range from single digits to tens of thousands, all of which would have experienced population crash events sometime in their history (Hamilton et al., 2014). Longitudinal data of indigenous population sizes gathered from direct census counts are incredibly rare in anthropology. These populations have primarily subsistence-based economies consisting of some combination of foraging, horticulture and agriculture. However, many of these populations will have experienced increasing interactions with market-based economies over time.

Administrative census of contacted populations

Demographic data for indigenous populations in Brazil derive primarily from administrative census systems operated by federal agencies, particularly the Fundação Nacional dos Povos Indígenas (FUNAI) and the Special Secretariat of Indigenous Health (SESAI). These data are subsequently compiled and systematized by the Instituto Socioambiental (ISA) through its *Povos Indígenas no Brasil* (PIB) database. The resulting dataset represents a longitudinal administrative census system for contacted indigenous populations (and an indirect monitoring system for isolated [uncontacted] groups, not reported here, but see Walker and Hamilton, 2014, 2019 and Walker et al., 2023).

For contacted indigenous societies, demographic data are collected through direct village-level population counts. The basic unit of enumeration is the village, typically located within legally recognized indigenous Lands (*Terras Indígenas*). FUNAI regional offices and SESAI health districts (*Distritos Sanitários Especiais Indígenas*, DSEIs) maintain local population records that are updated during routine administrative visits, health campaigns and special interventions.

Downloaded from https://www.cambridge.org/core. UNIVERSIDAD AUTONOMA METROPOLITANA, on 18 Nov 2026 at 04:05:37, subject to the Cambridge Core terms of use, available at https://www.cambridge.org/core/terms. https://doi.org/10.1017/ext.2026.10013

Village-level enumeration generally consists of complete counts of all residents physically present at the time of visit. Field agents record total population size and, in many cases, age and sex composition. These counts are transmitted to regional and national administrative databases. Because SESAI administers vaccination programs, primary care and epidemiological surveillance, health registries often function as continuously updated population lists.

There is no single synchronized national indigenous census cycle. Instead, the system operates as a rolling administrative census, with updates occurring at irregular intervals depending on logistical access, health activities and local conditions. National census operations conducted by the Brazilian Institute of Geography and Statistics (IBGE) provide additional cross-validation at decadal intervals, although discrepancies may arise due to seasonal mobility, urban migration and differences in ethnic self-identification.

Area estimates for populations also come from the Brazilian government and estimate the area assumed to be used by populations within indigenous protected areas, known as *Terras Indígenas*. These areas are not well-defined or demarcated, and may well overlap in many cases. Such areas will also be exploited in different ways, depending on the mobility and economics of each society. We do note, however, that despite measurement error, the relationship we report between area and population size for these Amazonian societies in these data is consistent with other more controlled studies of small-scale societies, where, in general, AN^{β} and $\beta < 1$ are often between 0.6 and 0.85 (Hamilton et al., 2007, 2020; Walker et al., 2014). Remarkably, we find similar spatial scaling relationships in a wide variety of human aggregations, including cities, both ancient and modern (Bettencourt et al., 2007; Ortman et al., 2020).

Enumeration following sustained peaceful contact

For groups undergoing their first sustained peaceful contact, population counts are typically conducted during or immediately after contact missions. Emergency health teams conduct rapid enumeration to assess population size and vulnerability to infectious disease. Follow-up counts are often conducted at relatively short intervals during the first 5–20 years after contact, when mortality risks are elevated and demographic volatility is greatest. These early post-contact series are particularly important for estimating contact-related mortality and subsequent rebound dynamics (Hamilton et al., 2014).

Data compilation and standardization

The ISA/PIB database functions as a centralized demographic repository. ISA compiles population figures from FUNAI, SESAI, IBGE and other official sources; standardizes ethnonyms; harmonizes geographic identifiers; and documents the year and source of each estimate. ISA does not conduct primary censuses but aggregates and systematizes official figures to produce publicly accessible time series. These data are released periodically and irregularly, as available.

Data characteristics and limitations

The principal strengths of this system are (i) reliance on full village counts rather than statistical sampling for contacted populations, (ii) multi-decade longitudinal depth and (iii) integration with health and administrative infrastructures. However, limitations include variable update frequency across regions, potential undercounting in highly mobile populations, political variability affecting data transparency and the inherently indirect nature of estimates for isolated groups. Cross-border populations may also be incompletely enumerated when censuses do not include communities located outside Brazil.

Due to the extreme sensitivity of the data, specific locations of the villages and populations are not available, limiting the ability to control for potential spatial autocorrelation or to examine other important ecological processes such as mobility, interaction networks or spatial synchrony.

Despite these limitations, the administrative census framework provides a robust empirical foundation for reconstructing contact mortality, estimating minimum viable population sizes, modeling post-contact growth trajectories and evaluating long-term demographic resilience in indigenous Amazonia.

Results

From the available data, we were able to calculate 1,353 instances of population growth. For each period of growth, we estimated the average annual growth rate over these time windows as

$$\widehat{r}_{i,t} = \left(\frac{1}{\Delta t}\right) \ln\left(\frac{N_{i,t+\Delta t}}{N_{i,t}}\right). \tag{6}$$

Figure 1A shows the distribution of population size estimates across the data set, and the inset is the average population size for each of the 227 populations. These distributions are approximately lognormal, as might be expected for populations generated by a multiplicative growth process (Hamilton and Walker, 2018). The median population size over all estimates is 414, and the median is 507.

Figure 1B shows the distribution of growth rate estimates (equation 6) across the data set, and the inset is the average growth rate for each of the 227 populations. The distribution is leptokurtic and non-normal, though approximately symmetrical. The average growth rate over all estimates is $\overline{r} = 0.032$ or 3.2% annual growth, and the median growth rate is $r_N = 0.039$, or 3.9%.

Figure 1C shows a funnel plot of the growth rate $\widehat{r}_{i,t}$ as a function of the corresponding population size $N_{i,t}$ at the beginning of the growth period. The inset figure is a plot of the average per population. Fitted OLS regressions (red lines) summarized in Table 1 show that growth rates are independent of population sizes, but are much more volatile at small population sizes.

Figure 1D shows the distribution of territory size estimates A in hectares (equation 6) across the data set. The distribution is approximately lognormal. The median territory size across populations is 2095 ha.

Figure 2A shows the log–log plot of the conditional standard deviation of growth rates, the volatilities, $\widehat{\sigma}(r|N_{\text{bin}})$ as a function of binned population sizes N_{bin}. A fitted OLS regression (red line) summarized in Table 2 shows that across populations, demographic volatility decreases with population size at a rate $\alpha = -0.26(-0.30, -0.21)$.

Figure 2B shows the log–log plot of the area of the territory size of a population as a function of the population size. A fitted OLS regression (red line) summarized in Table 3 shows that across populations, area scales positively with population size at a rate $\beta = 0.75$.

Downloaded from https://www.cambridge.org/core. UNIVERSIDAD AUTONOMA METROPOLITANA, on 18 Nov 2026 at 04:05:37, subject to the Cambridge Core terms of use, available at https://www.cambridge.org/core/terms. https://doi.org/10.1017/ext.2026.10013

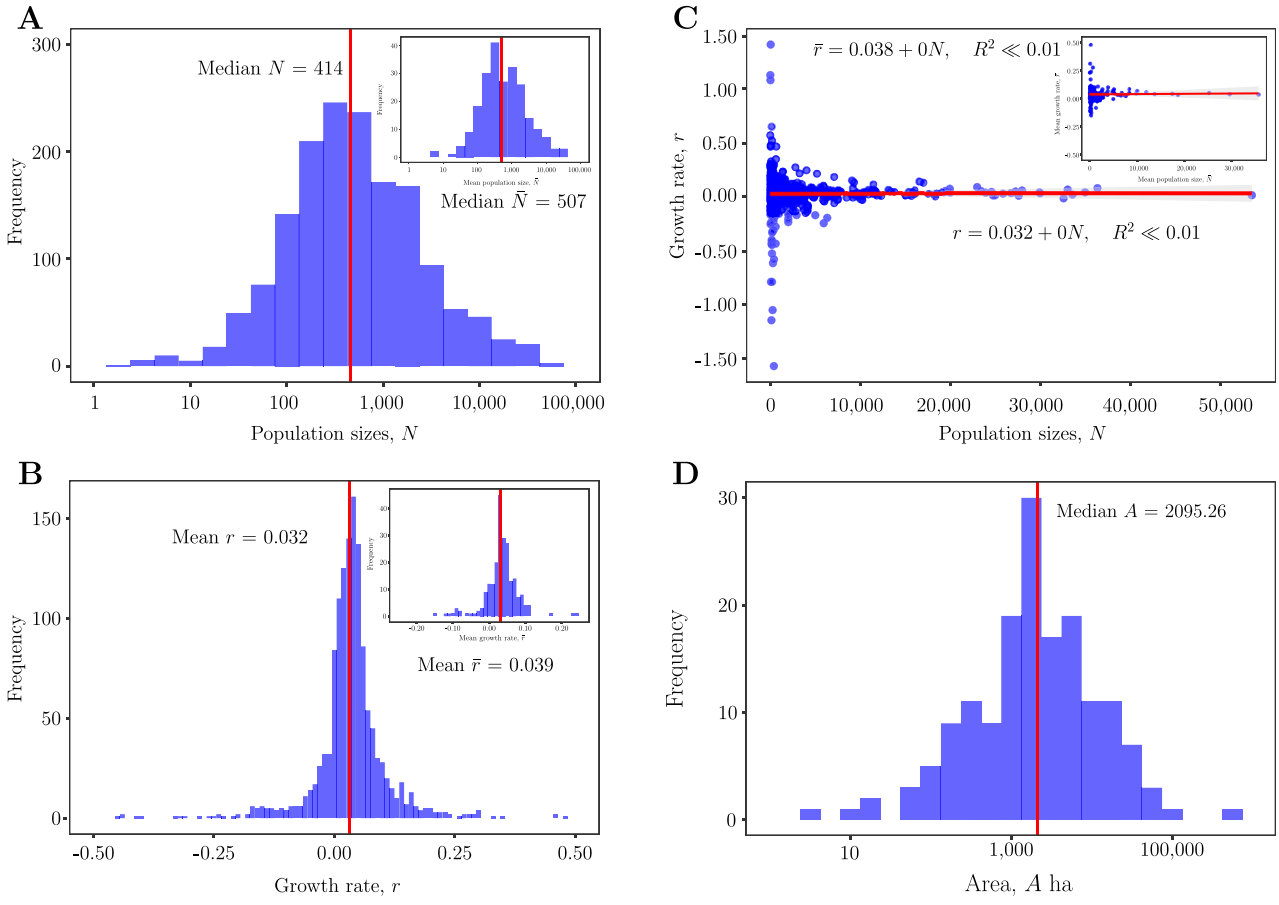


Figure 1. Population size and growth rates. (A) The distribution of all population size estimates from census populations is approximately lognormal with a median of 414 individuals. Inset in the upper right is the distribution of the average size of the 227 populations over their individual observation windows, with a median size of 507 individuals. (B) The distribution of all annual growth rates estimated from the census data (equation 6) with the mean growth rate $\bar{r} = 0.032$ or 3% per year (see Table 1. for details). Inset is the average growth rate for each of the 227 populations over their individual observation windows, with a mean growth rate $\bar{r}_N = 0.039$ or 4% per year. (C) Growth rate r as a function of population size N over all census estimates. The relationship shows a funnel plot typical of stochastic population dynamics where population volatility decreases with scale. Inset is the average growth rate of a population r_N as a function of the average population size $\overline{N}$. In both cases, population growth rates are not size-dependent. (D) The distribution of the geographic ranges, or areas A in hectares, for 161 of the 227 populations. The distribution is approximately lognormal with a median size of 2095.26 ha.

Table 1. Growth rate and population size scaling

	Dependent variable:
	r
$\widehat{r}_{i,t}$	–0.0000(−0.0000, 0.0000)
Constant	0.03*(0.03, 0.04)
Observations	1,353
R^2	0.0000
Residual std. error	0.12 (df = 1,351)
F statistic	0.004 (df = 1; 1,351)

Note: *$p < 0.01$

Synchrony scaling with N

Table 2 shows $\alpha = -0.26 \pm 0.05 \approx -1/4$ and so empirically $\sigma(r) \propto N^{-1/4} \Rightarrow \mathrm{Var}(r) \propto N^{-1/2}$. As such, volatility decays at half the rate expected by the baseline demographic model. For equation (3) to produce this result, synchrony (pairwise correlations) must decline with size as

$$\rho(N) \propto N^{-1/2}. \tag{7}$$

Then for large N, the synchrony term dominates:

$$\mathrm{Var}(r|N) \approx s^2 c_\rho N^{-1/2}, \Rightarrow \sigma(r|N) \propto N^{-1/4}, \tag{8}$$

matching the results we obtain from the data.

Further, these results suggest populations consist of effective correlated "clusters," or modular demographic units of average size $m(N) \propto N^{1/2}$. The effective number of independent draws is $K(N) \propto N^{1/2}$, yielding $\sigma(r) \sim K^{-1/2} \sim N^{-1/4}$. As such, volatility scales negatively with population size at half the rate of the baseline demographic model as pairwise correlations within populations dampen the rate at which stochasticity is averaged out by scale.

Link to space use and density

Table 3 shows $\beta = 3/4$. Since $A \propto N^{3/4}$, we have $A/N \propto N^{-1/4}$ and so $D = N/A \propto N^{1/4}$. Substituting into equation (8) we have,

$$\sigma(r) \propto N^{-1/4} = (N/A)^{-1} = D^{-1}. \tag{9}$$

Downloaded from https://www.cambridge.org/core. UNIVERSIDAD AUTONOMA METROPOLITANA, on 18 Nov 2026 at 04:05:37, subject to the Cambridge Core terms of use, available at https://www.cambridge.org/core/terms. https://doi.org/10.1017/ext.2026.10013

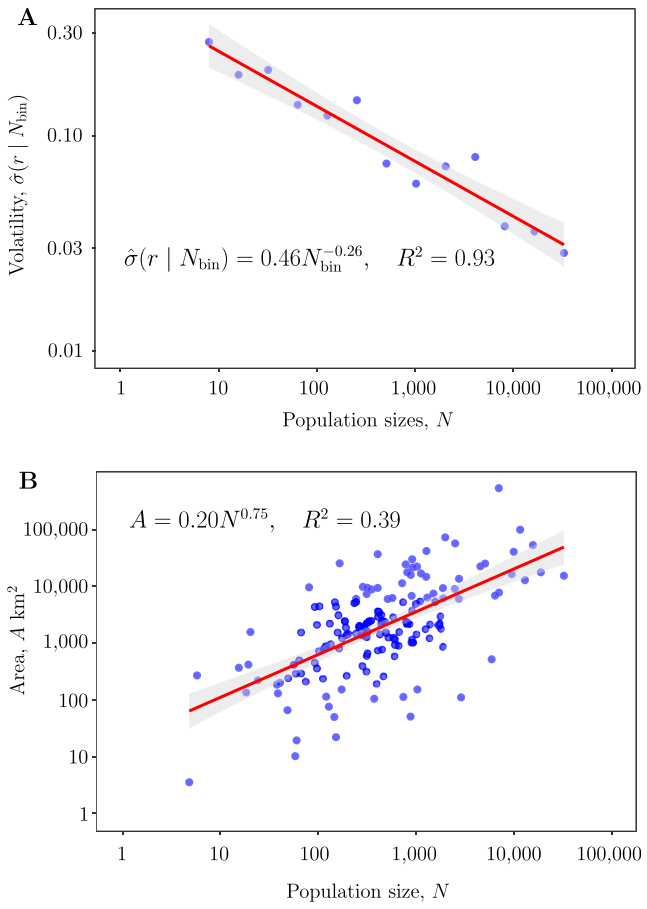


Figure 2. Demographic and population size area scaling. (A) Observed demographic volatility as a function of binned population size on a log-linear plot, following the methods outlined in the Methods section. Here, volatility declines with population size with a slope $\alpha = -0.26$ (see Table 2. for details). (B) The scaling of the area use A by population size N for 161 of our 227 populations (limited by data availability) on log–log axes. An OLS estimate of the relationship yields a sublinear slope of $\beta = 0.75$ (see Table 3. for details), as is commonly observed in the spatial ecology of traditional societies (Hamilton et al., 2007, 2012).

Table 2. Sigma scaling

	Dependent variable:
	$\widehat{\sigma}(r \mid N_{\text{bin}})$
α	–0.26*(–0.30,–0.21)
$\ln c$	–0.81*(–1.09,–0.53)
Observations	13
R^2	0.93
Residual std. error	0.20 (df = 11)
F statistic	142.78* (df = 1; 11)

Note: *$p < 0.01$.

Thus, population stability increases in direct proportion to population density.

Unified variance model

Conceptually, we can then define a full growth model composed of three terms:

Table 3. Area-population size scaling

	Dependent variable:
	lnA
β	0.75*(0.61,0.90)
Constant	2.99*(2.07,3.90)
Observations	160
R^2	0.39
Residual std. error	1.45 (df = 158)
F statistic	100.94* (df = 1; 158)

Note: *$p < 0.01$.

Table 4. Exponent mapping from spatial overlap to correlation and volatility

Quantity	Scaling relation	Implied exponent
Area use (per capita)	$A/N \sim N^{-1/4}$	$-1/4$
Population density	$D = N/A \sim N^{1/4}$	$1/4$
Pairwise correlation (synchrony)	$\rho(N) \sim N^{-1/2}$	$-1/2$
Variance of growth rate	$\text{Var}(r\|N) \sim N^{-1/2}$	$-1/2$
Volatility (std. dev.)	$\sigma(r) = N^{-1/4}$	$-1/4$
Density law of volatility	$\sigma(r) \sim D^{-1}$	-1

$$r = f(\text{individual contributions, demography, synchrony}). \quad (10)$$

We then formalize this into a general model that considers the effects of demography and synchrony (pairwise correlations) on population growth:

$$r_{i,t} = \mu_i - \phi \log N_{i,t} + \sigma_d N_{i,t}^{-1/2} \eta_{i,t} + \sigma_\rho N_{i,t}^{-1/4} \xi_{i,t}, \quad (11)$$

where ϕ is a density-dependence coefficient and both η and $\xi \sim \mathcal{N}(0,1)$. The conditional variance is then

$$\text{Var}(r|N) = \sigma_d^2 N^{-1} + \sigma_\rho^2 N^{-1/2}. \quad (12)$$

The observed scaling of volatility and space use shows that human demography is not reducible to independent births and deaths but is structured by social, ecological and institutional synchrony. Synchrony inflates volatility, but density, sharing and spatial organization counteract synchrony, stabilizing demographic trajectories. Table 4 summarizes this chain of exponents linking space use, correlation and volatility.

Data limitations and sources of uncertainty

As detailed above, our analyses rely on census time series that are short, irregularly spaced and heterogeneous in quality. Enumeration in remote indigenous regions is subject to logistical constraints, and even small counting errors can disproportionately affect growth rate estimates in small populations. Although random measurement noise may inflate volatility estimates, our inference depends primarily on how volatility scales with population size rather than on absolute variance levels.

It is also important to recognize that populations in the dataset are also not fully spatially independent. Neighboring groups often share climatic regimes, epidemiological exposure and broader

Downloaded from https://www.cambridge.org/core. UNIVERSIDAD AUTONOMA METROPOLITANA, on 18 Nov 2026 at 04:05:37, subject to the Cambridge Core terms of use, available at https://www.cambridge.org/core/terms. https://doi.org/10.1017/ext.2026.10013

ethnolinguistic networks, introducing spatial autocorrelation that may reduce effective sample size and increase parameter uncertainty. While such shared forcing is itself part of the synchrony process we seek to quantify, it complicates strict statistical independence assumptions. Unfortunately, we do not have access to spatial data to control for these effects, which would allow us to examine other aspects of ecological synchrony. However, we can only note that in similar studies of spatial ecology in small-scale human societies, spatial autocorrelation and other potentially confounding factors has had negligible impacts on empirically estimated scaling parameters (Hamilton et al., 2007, 2024).

In addition, demographic shocks, including epidemics, displacement and episodic contact events, introduce nonstationarity into growth rates. These rare but severe events contribute to observed volatility and could disproportionately influence scaling estimates. Finally, the synchrony-extended model assumes exchangeable pairwise correlations within populations, whereas real social systems likely exhibit heterogeneous network structures. The inferred effective modularity should therefore be interpreted as a coarse-grained approximation rather than a literal demographic partition. However, as above, we observe that empirical social network structures in small-scale societies are remarkably consistent in their size, modularity and hierarchical organization (Hamilton et al., 2007, 2020; Buchanan and Hamilton, 2023; Pablo et al., 2022). Despite these limitations, the consistent departure from classical $\sigma(r) \propto N^{-1/2}$ scaling suggests that independence is systematically violated. While parameter estimates carry uncertainty, the qualitative evidence for demographic synchrony remains robust across populations and regions.

Discussion

Using census data, we show that demographic synchrony at the individual scale inflates volatility at the population scale. Even numerically large human populations exhibit stochastic demographic fluctuations far greater than predicted under classical assumptions of independence. From an ecological perspective, this result challenges the long-standing premise that increasing population size alone guarantees stability through statistical averaging. Under independent demographic stochasticity, volatility in per-capita growth rates should scale as $\sigma(r) \propto N^{-1/2}$. Empirically, however, we observe $\sigma(r) \propto N^{-1/4}$. This systematic departure from independence indicates that individuals within populations do not behave as statistically independent demographic units. Instead, social organization induces demographic modularity as individuals are embedded within shared ecological and social environments, coupling their demographic outcomes.

There is no reason to assume that this result is a unique feature of human societies. On the contrary, we suggest it likely reflects a more general property of cooperative systems where cooperation reduces idiosyncratic risk by pooling resources, sharing labor and coordinating reproduction, yet the same mechanisms that buffer individuals against uncertainty introduce correlations among their demographic fates. In statistical terms, cooperation increases covariance while reducing individual variance. Because aggregate population variance depends on both variance and covariance, the latter becomes dominant as cooperation intensifies.

For example, our results suggest that a cooperative population of $N = 400$ individuals behaves demographically as if composed of only $K(N) \approx 20$ independent demographic units. The effective dimensionality of the population is dramatically reduced. Such dimensional collapse is precisely what one would expect in any cooperative organism in which reproduction, survival or resource acquisition is coordinated within modular social units, whether breeding pairs in wolves (Mech and Boitani, 2003; Smith et al., 2010), cooperative clusters in acorn woodpeckers (Koenig and Mumme, 1987; Joseph and Koenig, 2002; Koenig, 2002), dominant females in meerkat groups (Clutton-Brock et al., 1999, 2001) or colonies of eusocial insects (Bourke and Franks, 1995; Seeley, 2009). In each case, individuals do not experience independent risks; rather, they experience shared exposures.

In the model, pairwise correlation ρ captures the degree to which independence is violated. Ecologically, ρ represents shared environmental forcing and shared social exposure. Traditional, small-scale human populations are spatially clustered, often kin-structured, and socially integrated. Kinship, reciprocity and coordinated subsistence couple births and deaths across households (Hill and Hurtado, 2009; 2017; Gurven et al., 2000; Hill, 2002; Gurven, 2004; Kramer, 2010; Page et al., 2019; Kraft et al., 2021; Kraft et al., 2023). Fission–fusion mobility further synchronizes outcomes, as movement occurs in modular groupings rather than independently (Hill et al., 2011; Hill 2014; Hamilton et al., 2016; 2024). Environmental shocks, such as rainfall variability, prey fluctuations or crop failures, act simultaneously across co-resident households and pathogens propagate through dense interaction networks, synchronizing mortality, as well-documented in waves of post-contact epidemics decimating indigenous populations throughout Amazonia over the past 500 years (Ribeiro, 1967; Bodard, 1974; Hemming, 1978; Hurtado et al., 2001; Vaz, 2011; Hamilton et al., 2014).

These mechanisms of synchrony are general demographic processes in social species. In any cooperative species, shared nesting sites, communal dens, collective provisioning or reproductive skew couple demographic outcomes (Brown, 1987; Koenig and Mumme, 1987; Keller and Reeve, 1994; Creel and Macdonald, 1995; Clutton-Brock et al., 2001; Bourke, 2011). The ecological literature has long recognized that spatial synchrony among populations increases extinction risk by eroding rescue effects. Our findings demonstrate an analogous phenomenon *within* populations, as synchrony among individuals erodes internal stabilizing effects. Just as synchrony among subpopulations elevates regional extinction risk in metapopulations, synchrony among individuals elevates extinction risk within cooperative populations.

The synchrony-extended model formalizes this process. When $\rho = 0$, volatility declines as $\sigma(r) \sim N^{-1/2}$; when $\rho > 0$, the decay is slower, yielding the empirical scaling $\sigma(r) \sim N^{-1/4}$. The implied relationship $\rho(N) \sim N^{-1/2}$ suggests that correlations weaken with size, but only gradually. Populations become denser as they grow, with area scaling as $A \sim N^{3/4}$ and density $D \sim N^{1/4}$. Increasing density enhances both exposure coupling and buffering capacity. On one hand, shared space increases environmental synchrony; on the other, denser exchange networks redistribute risk. The net empirical outcome is $\sigma(r) \propto D^{-1}$, indicating that density weakens synchrony but does not eliminate it. In other words, larger populations are more stable because they are denser (Table 4), but the stabilizing effect of scale is weaker than expected under demographic independence due to increasing synchrony.

This dual role of density reveals the core tension of the cooperation–synchrony paradox. Cooperation evolved as a risk-pooling strategy, reducing individual variance in fitness-related outcomes. Yet cooperation simultaneously synchronizes exposure to large-scale shocks at the population level. Shared subsistence bases,

Downloaded from https://www.cambridge.org/core. UNIVERSIDAD AUTONOMA METROPOLITANA, on 18 Nov 2026 at 04:05:37, subject to the Cambridge Core terms of use, available at https://www.cambridge.org/core/terms. https://doi.org/10.1017/ext.2026.10013

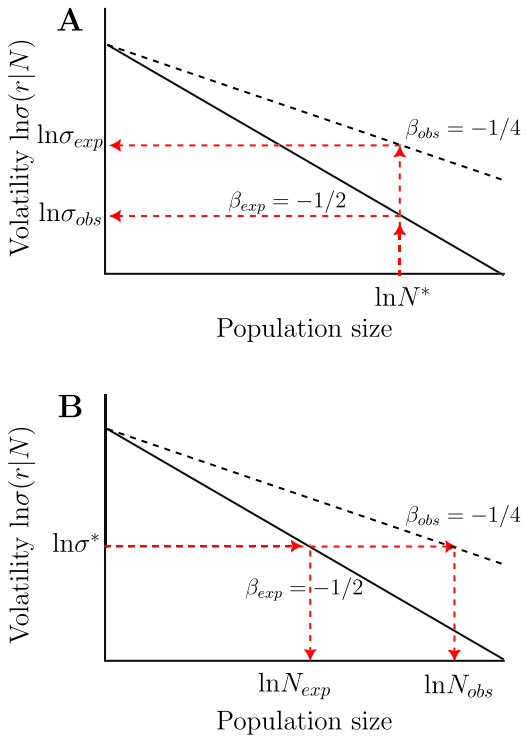


Figure 3. Demographic fluctuations schematic. (A) For a given population size, N^*, the expected volatility of the population σ_{exp} is lower than the observed volatility σ_{obs} as the observed slope $\beta_{obs} = -1/4$ is shallower than the expected slope $\beta_{obs} = -1/2$. (B) For a given level of volatility, σ^*, the expected population size N_{exp} is lower than the observed population size N_{obs}. As such, all populations are more volatile than expected for any given size, or equivalently, large populations are observed to be as volatile as smaller populations under the expected baseline demographic model.

coordinated reproduction and dense interaction networks mean that droughts, epidemics or regional disturbances impact all members simultaneously. Thus, cooperation stabilizes individuals while potentially increasing systemic fragility. This then begs the question: at what ecological scale does cooperation shift from buffering risk to amplifying shared vulnerability? And how does this vary across species populations that vary in their cooperative behaviors?

This trade-off mirrors well-known properties of tightly coupled systems in ecology and complex systems theory: systems that maximize local efficiency through integration often become more sensitive to correlated external shocks (May, 1972; Tilman et al., 1998; Scheffer et al., 2001; Watts, 2002; Loreau and de Mazancourt, 2008; Helbing, 2013). Cooperative populations occupy precisely this structural regime of high internal coupling, shared environmental exposure and reduced effective dimensionality.

The implications for extinction risk are substantial. Classical population viability analyses assume $\sigma^2(r) \propto 1/N$ and thus predict relatively modest minimum viable population sizes (Shaffer, 1981; Dennis et al., 1991; Morris and Doak, 2002; Traill et al., 2007). Under synchrony, however, minimum viable population sizes are roughly the square of baseline estimates. A population predicted to remain viable at $N_{\mathrm{MVP}} = 100$ under independence may require 10,000 under synchrony and so populations that appear demographically large enough to be secure may still be ecologically vulnerable (Figure 3B).

Conclusion

The synchrony-extended model thus formalizes a general ecological mechanism: when demographic events are correlated across individuals due to shared environments and social coupling, the stabilizing effect of size is weakened, volatility declines more slowly with N and extinction risk increases. In this view, the human case we document here is not anomalous but illustrative of a general demographic outcome. It provides a rare quantitative window into a broader ecological law of demography where scale does not guarantee stability when demographic fates are synchronized by shared ecologies and cooperation.

Open peer review. To view the open peer review materials for this article, please visit http://doi.org/10.1017/ext.2026.10013.

Supplementary material. The supplementary material for this article can be found at http://doi.org/10.1017/ext.2026.10013.

Data availability statement. All data used in this study are available as Supplementary Information attached to this paper.

References

Bettencourt LMA et al. (2007). Growth, innovation, scaling, and the pace of life in cities. *Proceedings of the National Academy of Sciences* **104**.(17), 7301–7306.

Bjørnstad ON, Ims RA and Lambin X (1999) Spatial population dynamics: Analyzing patterns and processes of population synchrony. *Trends in Ecology & Evolution* **14**(11), 427–432.

Bodard L (1974) *Green Hell: Massacre of the Brazilian Indians*. New York: Dutton.

Bourke AFG (2011) *Principles of Social Evolution*. Oxford: Oxford University Press.

Bourke AFG and Franks NR (1995) *Social Evolution in Ants*. Princeton: Princeton University Press.

Bowles S and Gintis H (2011) *A Cooperative Species: Human Reciprocity and its Evolution*. Princeton University Press.

Brown JL (1987) *Helping and Communal Breeding in Birds: Ecology and Evolution*. Princeton University Press.

Brown JH and Kodric-Brown A (1977) Turnover rates in insular biogeography: Effect of immigration on extinction. *Ecology* **58**(2), 445–449.

Buchanan B and Hamilton MJ (2023) Networks and cultural transmission in hunter-gatherer societies. In *The Oxford Handbook of Archaeological Network Research*. Oxford University Press.

Butzer KW (2012). Collapse, environment, and society. *Proceedings of the National Academy of Sciences* **109**.(10), 3632–3639.

Clutton-Brock T (2016) *Mammal Societies*. John Wiley & Sons.

Clutton-Brock TH, Philip NMB, O'Riain MJ, Gaynor G, Kansky R,Griffin AS and Manser M(1999) Selfish sentinels in cooperative mammals. *Science* **284**(5420), 1640–1644. https://doi.org/10.1126/science.284.5420.1640.

Clutton-Brock TH, Philip NMB, O'Riain MJ, Griffin A, Kansky R,Griffin A,Manser M,Sharpe L,McIlrath GM,Small T,Moss A and Monfort S(2001) Cooperation, control, and concession in meerkat groups. *Science* **291**(5503), 478–481. https://doi.org/10.1126/science.291.5503.478.

Creel S and Macdonald DW (1995) Sociality, group size, and reproductive suppression among carnivores. *Advances in the Study of Behavior* **24**, 203–257. https://doi.org/10.1016/S0065-3454(08)60353-1.

Cumming GS and Peterson GD (2017) Unifying research on social–ecological resilience and collapse. *Trends in Ecology & Evolution* **32**(9), 695–713. https://doi.org/10.1016/j.tree.2017.06.014.

Currie TE, Greenhill SJ, Gray RD, Hasegawa T and Mace R (2010) Rise and fall of political complexity in island South-East Asia and the Pacific. *Nature* **467**(7317), 801–804. https://doi.org/10.1038/nature09461.

Dennis B, Munholland PL and Scott JM (1991) Estimation of growth and extinction parameters for endangered species. *Ecological Monographs* **61**(2), 115–143.

Downloaded from https://www.cambridge.org/core. UNIVERSIDAD AUTONOMA METROPOLITANA, on 18 Nov 2026 at 04:05:37, subject to the Cambridge Core terms of use, available at https://www.cambridge.org/core/terms. https://doi.org/10.1017/ext.2026.10013

Diamond J (2011). *Collapse: How Societies Choose to Fail or Succeed:* revised edn. Penguin.

Earn, DJD, Rohani P, and Grenfell BT (1998). Persistence, chaos and synchrony in ecology and epidemiology. *Proceedings of the Royal Society of London. Series B: Biological Sciences* **265**.(1390), 7–10.

Gurven M (2004) To give and to give not: The behavioral ecology of human food transfers. *Behavioral and Brain Sciences* **27**(4), 543–560.

Gurven MD and Davison RJ (2019). Periodic catastrophes over human evolutionary history are necessary to explain the forager population paradox. *Proceedings of the National Academy of Sciences* **116**.26, 12758–12766.

Gurven M, et al. (2000) It's a wonderful life": Signaling generosity among the ache of Paraguay. *Evolution and Human Behavior* **21**(4), 263–282.

Hamilton MJ and Walker SR (2018) A stochastic density-dependent model of long-term population dynamics in hunter-gatherer populations. *Evolutionary Ecology Research* **19**(1), 85–102.

Hamilton MJ, **Milne BT**, **Walker RS**, **Burger O and Brown JH** (2007). The complex structure of hunter–gatherer social networks. *Proceedings of the Royal Society B: Biological Sciences* **274**.(1622), 2195–2203.

Hamilton MJ, **Burger O and Walker RS** (2012) Human ecology. In *Metabolic Ecology: A Scaling Approach*. Wiley-Blackwell, pp. 248–257.

Hamilton MJ, **Walker RS and Kesler DC** (2014) Crash and rebound of indigenous populations in lowland South America. *Scientific Reports* **4**(1), 4541.

Hamilton MJ, **Lobo J**, et al. (2016) The ecological and evolutionary energetics of hunter-gatherer residential mobility. *Evolutionary Anthropology: Issues, News, and Reviews* **25**(3), 124–132.

Hamilton MJ, **Walker RS**, **Buchanan B and Sandeford DS** (2020) Scaling human sociopolitical complexity. *PLoS One* **15**(7), e0234615. https://doi.org/10.1371/journal.pone.0234615.

Hamilton MJ, **Buchanan B**, et al. (2024) Food storage, mobility, and the density-dependence of hunter-gatherer movement ecology. *Journal of Archaeological Science: Reports* **54**, 104441.

Hamilton MJ, **Milne BT**, **Walker RS and Brown JH** (2007). Nonlinear scaling of space use in human hunter–gatherers. *Proceedings of the National Academy of Sciences* **104**.(11), 4765–4769.

Hanski I (1999) *Metapopulation Ecology*. Oxford University Press.

Helbing D (2013) Globally networked risks and how to respond. *Nature* **497**, 51–59. https://doi.org/10.1038/nature12047.

Hemming J (1978) *Red Gold: The Conquest of the Brazilian Indians*. Cambridge, MA: Harvard University Press.

Hill K (2002) Altruistic cooperation during foraging by the ache, and the evolved human predisposition to cooperate. *Human Nature* **13**(1), 105–128. https://doi.org/10.1007/s12110-002-1016-3.

Hill K and Hurtado AM (2009). Cooperative breeding in South American hunter–gatherers. *Proceedings of the Royal Society B: Biological Sciences* **276**.(1674), 3863–3870.

Hill K and Hurtado AM (2017) *Ache Life History: The Ecology and Demography of a Foraging People*. Routledge.

Hill KR, **Walker RS**, **Bozicević M**, **Eder J**, **Headland T**, **Hewlett B**, **Hurtado AM**, **Marlowe F**, **Wiessner P and Wood B** (2011) Co-residence patterns in hunter-gatherer societies show unique human social structure. *Science* **331**(6022), 1286–1289. https://doi.org/10.1126/science.1199071.

Hill KR, **Wood BM**, **Baggio J**, **Hurtado AM and Boyd RT** (2014) Hunter-gatherer inter-band interaction rates: Implications for cumulative culture. *PLoS One* **9**(7), e102806. https://doi.org/10.1371/journal.pone.0102806.

Hurtado M, **Hill K**, **Kaplan H and Lancaster J** (2001) The epidemiology of infectious diseases among south American Indians: A call for guidelines for ethical research. *Current Anthropology* **42**(3), 425–432. https://doi.org/10.1086/320005.

Instituto Socioambiental (2025). *Povos Indígenas no Brasil – Downloads*. https://pib.socioambiental.org/pt/Downloads. (accessed 28 September 2025)

Joseph H and Koenig WD (2002). Reproductive skew in the polygynandrous acorn woodpecker. *Proceedings of the National Academy of Sciences* **99**.(10), 7178–7183.

Keller L and Reeve HK (1994) Partitioning of reproduction in animal societies. *Trends in Ecology & Evolution* **9**(3), 98–102. https://doi.org/10.1016/0169-5347(94)90204-6.

Keyfitz N and Caswell H (2005) *Applied Mathematical Demography*. Springer.

Koenig WD (2002) Global patterns of environmental synchrony and the Moran effect. *Ecography* **25**(3), 283–288.

Koenig WD and Mumme RL (1987) *Population Ecology of the Cooperatively Breeding Acorn Woodpecker*. Princeton: Princeton University Press.

Kraft TS, **Venkataraman VV**, **Wallace IJ**, **Crittenden AN**, **Holowka NB**, **Stieglitz J**, **Harris J**, **Raichlen DA**, **Wood B**, **Gurven M**, **Pontzer H** (2021). "The energetics of uniquely human subsistence strategies". In: *Science* **374**.6575, eabf0130. https://doi.org/10.1126/science.abf0130.

Kraft TS, **Cummings DK**, et al. (2023) Female cooperative labour networks in hunter–gatherers and horticulturalists. *Philosophical Transactions of the Royal Society B* **378**(1868), 20210431.

Kramer KL (2010) Cooperative breeding and its significance to the demographic success of humans. *Annual Review of Anthropology* **39**, 417–436.

Krause J and Ruxton GD (2002) *Living in Groups*. Oxford University Press.

Lande R (1993) Risks of population extinction from demographic and environmental stochasticity and random catastrophes. *The American Naturalist* **142**(6), 911–927. https://doi.org/10.1086/285580.

Lande R, **Engen S and Sæther B-E** (1999) Spatial scale of population synchrony: Environmental correlation versus dispersal and density regulation. *The American Naturalist* **154**(3), 271–281. https://doi.org/10.1086/303240.

Lande R, **Engen S and Saether B-E** (2003) *Stochastic Population Dynamics in Ecology and Conservation*. Oxford: Oxford University Press.

Liebhold A, **Koenig WD and Bjørnstad ON** (2004) Spatial synchrony in population dynamics. *Annual Review of Ecology, Evolution, and Systematics* **35**(1), 467–490.

Loreau M and de Mazancourt C (2008) Species synchrony and its drivers: Neutral and nonneutral community dynamics in fluctuating environments. *The American Naturalist* **172**(2), E48–E66. https://doi.org/10.1086/589746.

May RM (1972) Will a large complex system be stable? *Nature* **238**(5364), 413–414. https://doi.org/10.1038/238413a0.

Mech LD and Boitani L (2003) *Wolves: Behavior, Ecology, and Conservation*. Chicago: University of Chicago Press.

Moran PAP (1953) The statistical analysis of the Canadian lynx cycle. *Australian Journal of Zoology* **1**(3), 291–298.

Morris WF and Doak DF (2002) *Quantitative Conservation Biology: Theory and Practice of Population Viability Analysis*. Sunderland, MA: Sinauer Associates.

Nowak MA (2006) Five rules for the evolution of cooperation. *Science* **314**(5805), 1560–1563. https://doi.org/10.1126/science.1133755.

Ortman SG, **Lobo J and Smith ME** (2020) Cities: Complexity, theory and history. *PLoS One* **15**(12), e0243621. https://doi.org/10.1371/journal.pone.0243621.

Pablo JF-L d, et al. (2022) Understanding hunter–gatherer cultural evolution needs network thinking. *Trends in Ecology & Evolution* **37**(8), 632–636.

Page AE, **Thomas MG**, **Smith D**, **Dyble M**, **Viguier S**, **Chaudhary N**, **Salali GD**, **Thompson J**, **Mace R and Migliano AB** (2019) Testing adaptive hypotheses of alloparenting in Agta foragers. *Nature Human Behaviour* **3**(11), 1154–1163. https://doi.org/10.1038/s41562-019-0679-2.

Ribeiro D (1967) Indigenous cultures and languages in Brazil. In Hopper J (ed), *Indians of Brazil in the Twentieth Century*. Washington, DC: Institute for Cross-Cultural Research, pp. 22–49.

Ricardo B and Ricardo F (1986) *Povos Indígenas no Brasil 1985/1986*. São Paulo: Instituto Socioambiental.

Ricardo B and Ricardo F (1991) *Povos Indígenas no Brasil 1987/1990*. São Paulo: Instituto Socioambiental.

Ricardo B and Ricardo F (1996) *Povos Indígenas no Brasil 1990/1995*. São Paulo: Instituto Socioambiental.

Ricardo B and Ricardo F (2000) *Povos Indígenas no Brasil 1996/2000*. São Paulo: Instituto Socioambiental.

Ricardo B and Ricardo F (2006) *Povos Indígenas no Brasil 2001/2005*. São Paulo: Instituto Socioambiental.

Ricardo B and Ricardo F (2011) *Povos Indígenas no Brasil 2006/2010*. São Paulo: Instituto Socioambiental.

Ricardo B and Ricardo F (2016) *Povos Indígenas no Brasil 2011/2015*. São Paulo: Instituto Socioambiental.

Ricardo B and Ricardo F (2023) *Povos Indígenas no Brasil 2016/2022*. São Paulo: Instituto Socioambiental.

Rubenstein DR (2011). "Spatiotemporal environmental variation, risk aversion, and the evolution of cooperative breeding as a bet-hedging strategy".

Downloaded from https://www.cambridge.org/core. UNIVERSIDAD AUTONOMA METROPOLITANA, on 18 Nov 2026 at 04:05:37, subject to the Cambridge Core terms of use, available at https://www.cambridge.org/core/terms. https://doi.org/10.1017/ext.2026.10013

Proceedings of the National Academy of Sciences **108** (Suppl 2), 10816–10822. https://doi.org/10.1073/pnas.1100303108.

Rubenstein DR and Lovette IJ (2007) Temporal environmental variability drives the evolution of cooperative breeding in birds. *Current Biology* **17**(16), 1414–1419. https://doi.org/10.1016/j.cub.2007.07.032.

Scheffer M, et al. (2001) Catastrophic shifts in ecosystems. *Nature* **413**, 591–596. https://doi.org/10.1038/35098000.

Schindler DE, **Hilborn R**, **Chasco B**, **Boatright CP**, **Quinn TP**, **Rogers LA and Webster MS** (2010) Population diversity and the portfolio effect in an exploited species. *Nature* **465**(7298), 609–612. https://doi.org/10.1038/nature09060.

Seeley TD (2009) *The Wisdom of the Hive: The Social Physiology of Honey Bee Colonies*. Harvard University Press.

Shaffer ML (1981) Minimum population sizes for species conservation. *Bioscience* **31**(2), 131–134. https://doi.org/10.2307/1308256.

Smith DW, **Stahler DR and Guernsey DS** (2010) Survival of colonizing wolves in the northern Rocky Mountains of the United States, 1982–2004. *Journal of Wildlife Management* **74**(4), 620–634. https://doi.org/10.2193/2008-584.

Stanley MHR, et al. (1996) Scaling behaviour in the growth of companies. *Nature* **379**(6568), 804–806.

Tainter J (1988) *The Collapse of Complex Societies*. Cambridge University Press.

Tilman D, **Lehman CL and Bristow CE** (1998) Diversity-stability relationships: Statistical inevitability or ecological consequence? *The American Naturalist* **151**(3), 277–282. https://doi.org/10.1086/286118.

Traill LW, **Bradshaw CA, and Brook BW** (2007). "Minimum viable population size: A meta-analysis of 30 years of published estimates". *Biological Conservation* **139**.(1–2), 159–166.

Turchin P (2018) *Historical Dynamics: Why States Rise and Fall*. Princeton University Press.

Vaz A (2011). Isolados *no Brasil. Política de Estado: da tutela para a política de direitos – uma questão resolvida*? Brasília: Estação Gráfica.

Walker RS and Hamilton MJ (2011). Social complexity and linguistic diversity in the Austronesian and Bantu population expansions. *Proceedings of the Royal Society B: Biological Sciences* **278**.(1710), 1399–1404.

Walker RS and Hamilton MJ (2014) Amazonian societies on the brink of extinction. *American Journal of Human Biology* **26**(4), 570–572. https://doi.org/10.1002/ajhb.22552.

Walker RS and Hamilton MJ (2019) Machine learning with remote sensing data to locate uncontacted indigenous villages in Amazonia. *PeerJ Computer Science* **5**, e170.

Walker RS, **Hamilton MJ and Groth AA** (2014) Remote sensing and conservation of isolated indigenous villages in Amazonia. *Royal Society Open Science* **1**(3).

Walker RS, **Flinn MV**, **Prall SP and Hamilton MJ** (2023) Remote sensing evidence for population growth of isolated indigenous societies in Amazonia. *Scientific Reports* **13**(1), 22448. https://doi.org/10.1038/s41598-023-50127-y.

Watts DJ (2002). A simple model of global cascades on random networks. *Proceedings of the National Academy of Sciences* **99**.9, 5766–5771. https://doi.org/10.1073/pnas.082090499.

Downloaded from https://www.cambridge.org/core. UNIVERSIDAD AUTONOMA METROPOLITANA, on 18 Nov 2026 at 04:05:37, subject to the Cambridge Core terms of use, available at https://www.cambridge.org/core/terms. https://doi.org/10.1017/ext.2026.10013